

Ni incorporation in pSOFC anode ceramic matrix: Part II. Wet chemical reduction in an anhydrous medium

M. V. Gabrovska^{1*}, D. A. Nikolova¹, E. A. Mladenova², D. E. Vladikova²,
S. K. Rakovsky¹, Z. B. Stoynov^{2†}

¹*Institute of Catalysis, Bulgarian Academy of Sciences, Acad. G. Bonchev Str., Bldg. 11,
1113 Sofia, Bulgaria*

²*Acad. Evgeni Budevski Institute of Electrochemistry and Energy Systems, Bulgarian Academy of Sciences, Acad. G.
Bonchev Str. Bldg. 10, 1113 Sofia, Bulgaria*

Received May 26, 2017; Accepted September 25, 2017

The well-known proton conductive electrolyte yttrium-doped barium cerate $\text{BaCe}_{0.85}\text{Y}_{0.15}\text{O}_{2.925}$ (BCY15) was used as an anode ceramic matrix for synthesis of Ni-based cermet anode with application in proton conducting solid oxide fuel cell (pSOFC). A cost-effective and energy-efficient wet-chemical reduction approach was presented by using of nickel chloride hexahydrate as precursor, ethylene glycol as anhydrous medium, hydrazine hydrate as reducing agent and alkaline solution as pH regulator. The characterization of the Ni-cermet was performed by Powder X-ray diffraction, N_2 -physisorption and SEM techniques. The electrochemical properties of anode cermet were determined by impedance spectroscopy after high-temperature sintering followed by reduction in hydrogen atmosphere. It was found that the preparation of BCY15/Ni cermet in ethylene glycol medium leads to (i) Structure preservation of the proton conducting ceramic matrix in the anode composite; (ii) Increase the specific surface area as result of metal Ni phase formation, a precondition for existence of numerous active sites for fuel electrochemical oxidation; (iii) Obtaining of homogeneous, nano-scaled, uniform distributed and non-agglomerated metal nickel particles. The cermet elaborated by ethylene glycol assisted route possesses a capacity to be promising anode in BCY-based pSOFC devices because of the anode ceramic matrix structure preservation and demonstrated electrochemical performance.

Keywords: BCY15/Ni anode cermet; Ethylene glycol; Hydrazine; PXRD; SEM; Electrochemical impedance spectroscopy.

INTRODUCTION

The anodes for protonic solid oxide fuel cells (pSOFC) are often applied as composites (mixtures) of the electron conducting electrode material and the proton conducting electrolyte. One of the most commonly used anode for hydrogen oxidation is a porous cermet structure consisting of two interpenetrating and interconnecting networks of Ni-metal and electrolyte particles. Yttrium-doped barium cerate $\text{BaCe}_{1-x}\text{Y}_x\text{O}_{3-\delta}$ (BCY) with ABO_3 perovskite-type structure is known as a widely applicable solid proton conductive electrolyte [1-5].

Generally, the anode cermet is fabricated by incorporation of NiO in the BCY electrolyte, applying standard ceramic technology, namely mixing, cold pressing and sintering, followed by reduction of the anode before operation of the cell. The low kinetics and high temperature, typical for this approach results in obtaining of solids with low homogeneity, presence of undesired secondary phases and uncontrolled (and typically large) particle size of low surface area [6]. Another

complication is the eventual formation of parasitic phases at the electrode/electrolyte interfaces that can limit the ionic migration, thereby increasing the electrode polarization [7].

It was reported that the formation of small-sized Ni particles in the Ni/YSZ cermet promotes the development of fine continuous Ni network and results in improvements in electrical conductivity and porosity [8]. The existence of small Ni^0 particles will provide for generation of numerous catalytic sites for the hydrogen adsorption provoking the enhancement of the anode activity. Thereby, the usage of synthesis modes for preparation of nano-sized metal nickel particles is one of the solutions for better efficiency of the anode cermet [9].

The preparation of fine nickel powders has been investigated intensively by the reduction of nickel salts in aqueous solution due to the good solubility of nickel salts in water, the low reaction temperature and the simple procedure [10]. A successful synthesis route represents the wet-

* To whom all correspondence should be sent.
E-mail: margo@ic.bas.bg

reduction mode, using hydrazine (N_2H_4) where the morphology of nickel powders, such as the shape and the size of particles, the size distribution and the degree of agglomeration, can be easily controlled by the reaction parameter, the solvent composition, the nucleation agent, the surfactant, etc. [11-14]. Hydrazine is attractive reducing agent for the preparation of fine nickel powder due to its strong reduction properties in low temperature range and high pH values. The temperature and pH dependence of hydrazine reducing ability makes the synthesis easily controllable [15, 16].

Hydrazine has a standard reduction potential of $-1.16V$ in an alkaline solution, represented by the oxidation reaction ($N_2H_4 + 4OH^- = N_2 + 4H_2O + 4e^-$) [15, 17]. Nickel, which has a standard reduction potential of $-0.25V$, is consequently able to be reduced by N_2H_4 ($2Ni^{2+} + 4e^- = 2Ni$) [15]. Therefore, a chemical reduction of the Ni^{2+} ion with N_2H_4 in basic environment at high pH (favorable to form pure Ni nanoparticles) [14, 15] can be simply shown in the following equation: $2Ni^{2+} + N_2H_4 + 4OH^- \rightarrow 2Ni + N_2 + 4H_2O$. The reduction is accompanied by gaseous nitrogen evolution, followed by growth of Ni^0 particles. The degree of reduction can be determined from the nitrogen volume according to the above mentioned reaction. Solution pH influences the synthesis of the nickel nanoparticles. The discharge of the nickel nanoparticles is enhanced when the redox potential increases because of the increasing pH of the solution, by adding a strong base at a certain temperature and constant nickel ion concentration. In addition, it has been shown that black nickel powder, cannot be produced if the pH is less than 9.5 [14, 15].

In our previous paper [18] the metal Ni was incorporated in the anode ceramic matrix of yttrium-doped barium cerate, $BaCe_{0.85}Y_{0.15}O_{2.925}$ (BCY15) by wet-chemical approach as an alternative to the traditional ceramic method for pSOFC Ni-based cermet anode preparation. The possibility of metal Ni incorporation in BCY15 by wet-chemical reduction with hydrazine route in an aqueous medium was examined. It was found that Ni-anode cermet demonstrated electrochemical performance similar to that of commercial NiO-based anode cermets in respect to the electronic conductivity of the Ni net. It was established that the preparation of Ni-cermet anode precursor in an aqueous medium results in partial reorganization of the initial BCY15 structure due to the hydrophilic properties of the used ceramic matrix.

Another approach for synthesis of nickel nanoparticles is the reduction with hydrazine in an anhydrous environment [19]. In this regard, in the so-called polyol process (polyol is an alcohol containing functional OH groups), the ethylene glycol (EG) as monomeric polyol serves as both reducer and solvent. EG with a relatively high boiling point ($198^\circ C$) is a good dispersive medium for starting reactants and as a good capping agent with two OH groups, it can hold free metal ions tightly in the solution [20, 21]. No metal Ni particles can be formed in EG medium without adding sufficient amount of hydrazine indicating that Ni^{2+} ions are reduced by hydrazine instead of EG.

It can be expected that if the incorporation of Ni in pSOFC anode ceramic matrix is performed in EG medium a preservation of the anode ceramic matrix in the BCY15/Ni cermet may be achieved.

EXPERIMENTAL

Sample preparation

BCY15/Ni-EG sample with a composition of NiO/BCY15 = 44.4/55.6 (volume ratio) was synthesized in non-aqueous surroundings by means of Ethylene glycol anhydrous, 99.8% acquired by SIGMA-ALDRICH. More detailed description of the preparation procedure was presented in Ref. 18. Briefly, this technique consists in obtaining of BCY15/Ni cermet precursor powder by chemical reduction of $NiCl_2$ with hydrazine. The role of EG is to prevent a high affinity of BCY15 to water.

To get reference sample for the characterization of BCY15/Ni-EG, unsupported nickel denoted as Ni-EG, was also prepared in the same manner, however in the absence of the anode ceramic matrix.

Sample characterization

Powder X-ray diffraction (PXRD) data were collected on an APD 15 Philips 2134 diffractometer employing $CuK\alpha$ radiation ($\lambda = 0.15418$ nm), operated at $U = 40$ kV and $I = 30$ mA. The crystalline phases were identified using Joint Committee on Powder Diffraction Standards (JCPDS) files.

The morphological studies were performed using Electron microscope JEOL 6390 equipped with INCA Oxford an energy dispersive X-ray spectroscopy (EDS).

The texture characteristics were determined by low-temperature ($77.4K$) nitrogen adsorption in a Quantachrome Instruments NOVA 1200e (USA) apparatus. The nitrogen adsorption-desorption isotherms were analyzed to evaluate the specific surface area, determined on the basis of the BET

equation. The samples were outgassed for 16 h in vacuum at 80°C before the measurements.

For *in situ* analysis of the Ni network performance an impedance approach for direct measurements of the Ni cermet electronic conductivity in the classical Ni-YSZ was applied [22]. The electrochemical impedance measurements were performed on IVIUM - CompactStat e10030 in the temperature interval 100–750°C and frequency range 1 MHz–0.01 Hz with a density of 5 points/decade and amplitude of the AC signal 1 mA in reduction atmosphere. The testing is performed on single “bare” anodes sandwiched between two Ni contact nets. The direct analysis starts in the beginning of the reduction stage at 750°C. In this way, the electronic conductivity is directly measured giving accurate information regarding the nickel network formation in the bulk anode structure.

RESULTS AND DISCUSSIONS

The PXRD patterns of BCY15 (Fig. 1a) show the presence of a single phase that can be attributed to orthorhombic perovskite, isostructural with BaCeO₃ (JCPDS file 00-022-0074) and yttrium doped analogue, BaCe_{0.9}Y_{0.1}O_{2.95} (JCPDS file 01-081-1386). The recorded well-formed reflections BaCeO₃ are in agreement with the calculated mean crystallite size of 150 Å. No diffraction peaks due to Y₂O₃ phase are registered indicating that yttrium ions are incorporated into the perovskite lattice [18].

As it can be seen from the diffractogram of BCY15/Ni-EG (Fig. 1b), the typical reflections of the metal Ni with cubic lattice symmetry (fcc) according to standard of metal Ni (JCPDS file 00-004-0085) and reference patterns of sample Ni-EG (Fig. 1c) are observed. Furthermore, the respective 2θ angles of the characteristic peaks of BCY15 in the BCY15/Ni-EG sample have no changes compared to the original BCY15 perovskite, indicating that no excrement reactions taken place during the BCY15/Ni-EG preparation and good chemical compatibility between the BCY15 and metal Ni.

The calculated metal Ni lattice parameter (*a*) and the metal Ni cell volume (*V*_{cell}) of BCY15/Ni-EG are presented in Table 1, displaying values similar to those of standard metal Ni (JCPDS file 00-004-0850). A difference in the intensity of the metal Ni reflections going from BCY15/Ni-EG to unsupported reference Ni-EG sample is detected, showing a different degree of crystallinity.

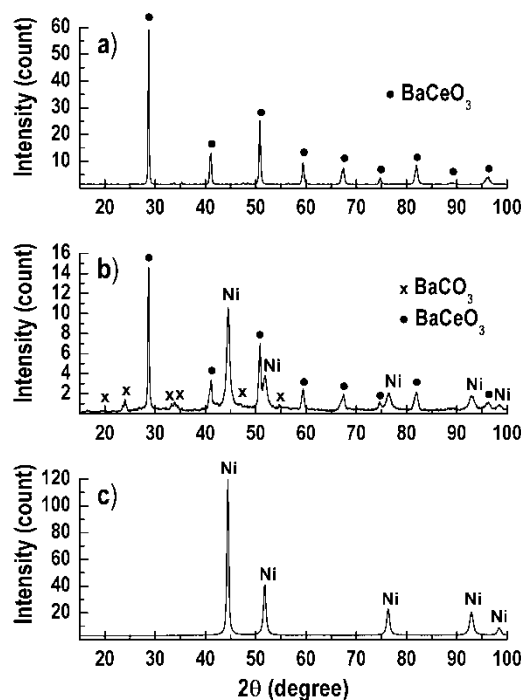


Fig. 1. PXRD patterns of BCY15 (a), BCY15/Ni-EG (b) and Ni-EG (c) solids

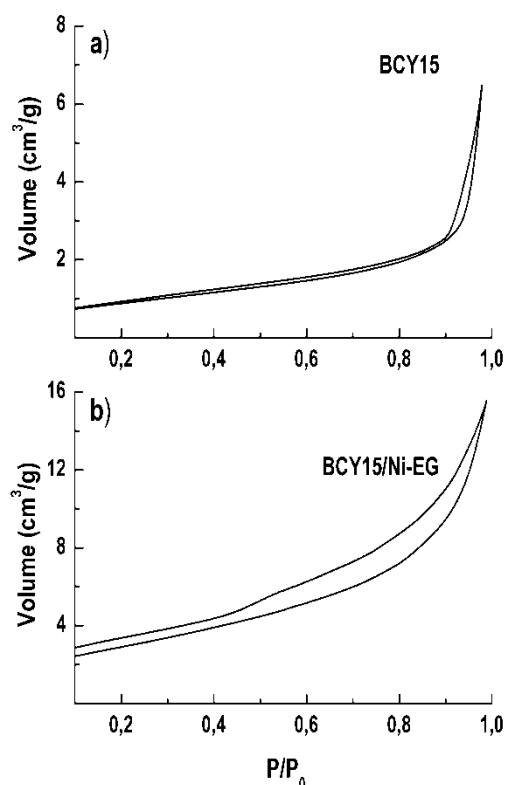
The positive role of the BCY15 presence in the anode composite on the metal nickel dispersion is clearly demonstrated by the values of the bulk mean Ni⁰ crystallite sizes (*L*) estimated from the full-width at half-maximum value of the most intensive peak of the Ni⁰ phase (111) situated at 2θ ≈ 44.5°. The data collected in Table 1 discloses the smaller size of metal Ni crystallites in BCY15/Ni-EG (130 Å) in comparison with those of unsupported reference sample Ni-EG (220 Å). On another hand, the smaller mean Ni⁰ crystallite size of BCY15/Ni-EG than that one in analogue sample, prepared in water (157 Å) [18] illustrates the dispersive role of EG medium.

Well-organized reflections of orthorhombic BaCeO₃ phase are also recorded with the as-prepared BCY15/Ni-EG (Fig. 1b) as opposed to the sample prepared in water [18]. PXRD analysis unveils only a few low intensity reflections of BaCO₃ phase with orthorhombic lattice symmetry (JCPDS file 00-045-1471). The observed phenomenon evidences for the preservation of the ceramic matrix BCY15 structure during synthesis of the Ni-based anode sample in EG environment.

Table 1. Lattice parameters of metal Ni and NiO obtained after treatment of BCY15/Ni-EG in different atmospheres

Parameter	BCY15/Ni-EG			Reference	JCPDS files
	as-prepared ^a	sintered ^b	post-impedance ^a	^a Ni ⁰ (00-004-0850)	^b NiO (00-047-1049)
<i>a</i> (Å)	3.5056(15)	4.1788(17)	3.5269(9)	3.5238	4.1771
<i>V</i> _{cell} (Å ³)	43.083(56)	72.97(11)	43.87(34)	43.76	72.88
<i>L</i> (Å)	130.0(92)	153.0(27)	248.1(19)	-	-

N₂-physisorption analysis reveals that BCY15 anode matrix is a typical macroporous material such is confirmed from type of its isotherm (Fig. 2a), II Type characteristic of aggregated powders as clays, cements, etc. [23].

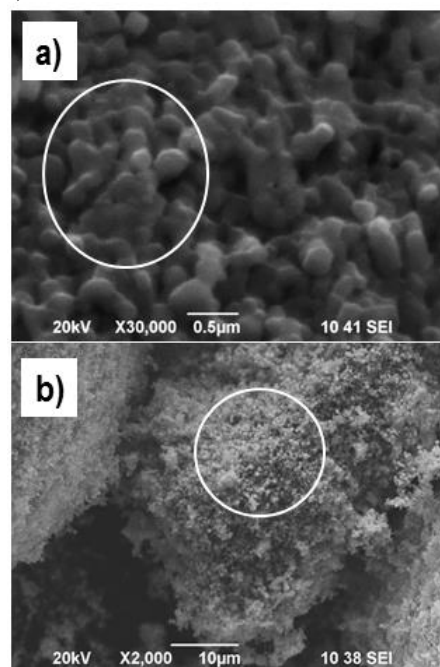
**Fig. 2.** Adsorption–desorption isotherms of BCY15 (a) and BCY15/Ni-EG (b) solids

The observed very narrow hysteresis loop displays presence of some mesopores on the surface which are termed as Type IIb exhibiting Type H3 hysteresis. Type H3 hysteresis loop is a distinctive of aggregates of platy particles or adsorbents containing slit-shapes pores [23].

The character of the isotherm type is preserved after incorporation of Ni²⁺ ions subsequent by reduction to the metal Ni state (Fig. 2b). The clearly detected hysteresis (H3 type) for BCY15/Ni-EG confirms generation of new mesopore system from metal nickel phase on BCY15. This finding corresponds to increase in the BET surface area from 3 m²/g for BCY15 to 11 m²/g. The three and a half times increase in BET surface area is a

precondition for existence of numerous surface active sites where the electrochemical fuel oxidation is carried out.

The microstructure observations by SEM indicate that anode matrix BCY15 possesses relatively homogeneous porous structure. The powder surfaces consist of randomly distributed particles similar in kind and shape (Fig. 3a). The deposition of metal nickel on BCY15 surface does not altered the morphology of the ceramic matrix (Fig. 3b).

**Fig. 3.** SEM micrographs of BCY15 (a) and BCY15/Ni-EG (b) solids

The image of BCY15/Ni-EG show easily recognizable mono-dispersed spherical Ni⁰ particles (Fig. 3b). The surface is composed of identical in shape fine-grained particles signifying that the synthesis in EG medium induces obtaining of precursor with smaller particle size than in water. It may be remarked also that single independent fragments of BCY15 anode matrix are not recorded on the surface of BCY15/Ni-EG as in the case of the analogue sample prepared in water [18]. This result prompts higher sample homogeneity and uniform distribution of the metal

nickel particles on the perovskite phase in BCY15/Ni-EG.

The surface elemental analysis performed by Energy Dispersive Spectroscopy (EDS) is presented

Table 2. The surface elemental analysis of the studied solids

Element (wt. %)	O	Ni	Ba	Ce	Y	Ba/Ce
BCY15	16.54	-	42.34	36.95	4.17	1.145
BCY15/Ni-EG	10.99	62.44	13.38	11.84	1.35	1.130

The characterization data suggest that the preparation of supported on BCY15 Ni-based cermet anode by EG assisted synthesis approach leads to the preservation of the proton conducting ceramic matrix in the anode composite. The metal Ni phase provides the required catalytic activity and electronic conductivity for the oxidation of hydrogen fuel. It is of significant importance the existence of BCY15 phase in the cermet because it plays an essential electrocatalytic role in the creation of additional reaction sites where the anode reactions may occur, providing a conductivity network for H⁺ ions and extends the triple-phase boundary (TPB) length, thereby resulting in improved electrode performance in addition to the inhibiting of the coarsening and grain growth of the metal Ni particles [1, 7, 24].

For analysis of the Ni network quality in the structure of a real anode, the standard ceramic technology was used for the preparation of pressed tablets from BCY15/Ni-EG (cold pressing, 3t/5 min), followed by their sintering in air at 1200°C for 5 h. The volumetric shrinkage of the tablet didn't exceed 6%. Because the NiO phase is reduced to the metal Ni in a separate step, the sintering of cermet at lower temperatures than 1200°C can induce poor performance due to poor connectivity in the electrolyte.

PXRD patterns of sintered BCY15/Ni-EG (Fig. 4a) exhibits thin and intensive reflections of well-crystallized NiO phase with lattice parameters (*a* and *V_{cell}*) close to the standard NiO (JCPDS file 00-047-1049) (Table 1). Well-defined diffraction lines of BaCeO₃ phase are also detected, signifying presence/preservation of the perovskite structure. Furthermore, an appearance of very low in intensity diffraction lines characteristics for orthorhombic Y₂BaNiO₅ oxide phase is documented (JCPDS file 00-047-0090). Likewise, a poorly crystallized BaNiO_{2.36} phase with hexagonal crystal symmetry (JCPDS file 00-047-0089) was identified in sintered sample, prepared in water [18]. Similar results was reported for sintered BZY20/NiO proton conducting ceramic which contains second-impurity phases as BaNiO_x (2 < x < 3) and Y₂BaNiO₅, that host unincorporated Ni²⁺ ions into BZY [25].

in Table 2. The marked areas in both images documented the presences of all the elements from the sample composition. The Ba/Ce ratio evidences the preservation of BCY15 structure.

A comparison of the NiO mean particle size shows larger values in BCY15/Ni-EG (153 Å) than that one in analogue sample, prepared in water (124 Å) [18] which corresponds with the better crystallization of NiO phase in BCY15/Ni-EG. Nevertheless, it may be noted that the sintering prompts formation of nano-metric NiO particles (Table 1) dispersed over the BCY15 matrix.

The next stage for BCY15/Ni-EG cermet formation represents a step-wise standard reduction procedure, performed at 750°C with a H₂/N₂ gaseous mixture. The first reduction step was accomplished with gaseous mixture of N₂ (flow rate of 35 nml/min·cm⁻²) and gradually increasing portions of H₂ (flow rate of 10 nml/min·cm⁻²). This treatment results in reduction of NiO surface until to formation of the Ni net. The second reduction step concerns treatment only with H₂ gas (flow rate of 35 nml/min·cm⁻²) for 60 min.

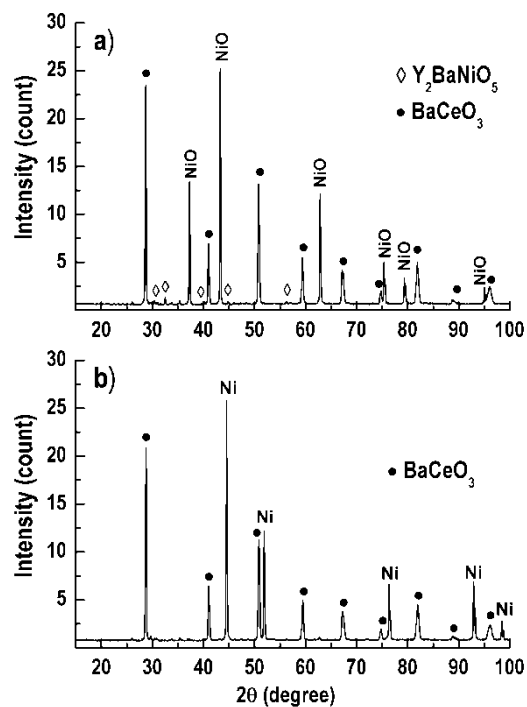


Fig. 4. PXRD patterns of BCY15/Ni-EG after sintering (a) and after impedance measurements (b)

The impedance measurements shows that prior to the reduction (0 min) the resistance of

BCY15/Ni-EG is changed in large interval from 180 to 215 Ω (Fig. 5a) in comparison with the cermet prepared in water that demonstrates a fairly low resistance of 31.5 Ω [18].

The reduction of BCY15/Ni-EG (Fig. 5b) starts at 11 min after the beginning of the process and displays similar resistivity to the cermet, synthesized in water medium, which reduction starts at 8 minute [18]. The reduction progression of BCY15/Ni-EG proceeds slowly and after 37 minutes from the beginning of the reduction, the resistance of Ni net drops down to 52 m Ω . The resistivity value remains unchanged until the end of the reduction cycle of 137 minutes. Inversely, the reduction of cermet prepared in water advances more rapidly thus the resistance of Ni net decreases down to 70 m Ω for about 20 minutes and remains unchanged until the end of the reduction cycle of 123 minutes [18].

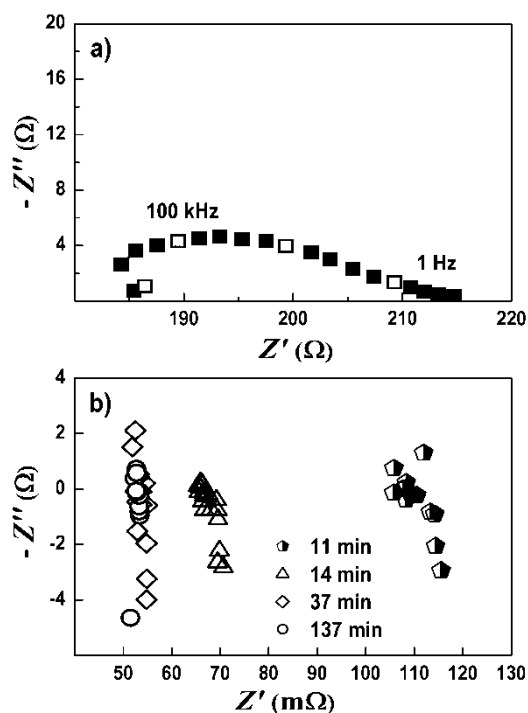


Fig. 5. Impedance diagrams measured during the reduction of BCY15/Ni-EG cermet before the beginning of the reduction (a) and after 11, 14, 37 and 137 minutes of reduction (b)

A comparative analysis allows to be noted that BCY15/Ni-EG exhibits improved electrochemical performance than the analogue cermet synthesized in water because at the end of reduction cycle, the resistivity of BCY15/Ni-EG reaches lower value than the prepared in water cermet.

A possible explanation of the demonstrated electrochemical behavior may be found in the results obtained from PXRD experiments of the sintered and post-impedance (reduced) cermets.

Sintering of the cermet prepared in water leads to the obtaining of rather complex material consisting of NiO and BCY15 perovskite as prevailing phases, and BaNiO_{2.36} and Y_{0.10}Ce_{0.90}O_{1.95} as impurity phases [18]. After reduction/impedance, reflections of metal Ni along with these corresponding to BaCeO₃, BaNiO_{2.36} and Y_{0.10}Ce_{0.90}O_{1.95} phases were registered. The existence of hexagonal BaNiO_{2.36} phase indicates that the incorporated Ni ions into BaNiO_{2.36} cannot be reduced to the metal state at temperature of 750°C. This explains a shorter time of about 20 minutes needed for reduction only of the Ni²⁺ ions included in the NiO phase.

The relatively slow reduction of sintered BCY15/Ni-EG (37 minutes) may be ascribed to the reduction of Ni²⁺ ions from dominant NiO phase assisted by the reduction of Ni²⁺ ones that exist within the Y₂BaNiO₅ second-phase (Fig. 4a).

PXRD patterns of post-impedance BCY15/Ni-EG cermet (Fig. 4b) displays only reflections of well-organized cubic metal Ni along with BCY15 perovskite structure. Apparently, the Ni²⁺ ions incorporated in Y₂BaNiO₅ second-phase are completely reduced to the metal Ni suggesting high purity and absence of parasitic phases which may affect the cermet conductivity. The results obtained demonstrate the advantage of the EG assisted synthesis method.

The calculated metal Ni lattice parameter values of post-impedance BCY15/Ni-EG cermet are comparable to these of the standard metal Ni (Table 1). The estimation of the mean metal Ni crystallite sizes (L) from the full-width at half-maximum values of the (111) diffraction lines at 2 θ \approx 44.5° reveals that the reduction/impedance causes growth of the initial metal Ni crystallites being also in nano-metric scale.

The slightly longer reduction time for BCY15/Ni-EG cermet induces formation of relatively larger metal Ni particles (248 Å) in comparison with these one of the cermet prepared in water (231 Å) [18].

CONCLUSIONS

The synthesis of Ni cermet in non-aqueous medium preserves the proton conducting ceramic structure in the anode composite thus suppresses the thermally induced coarsening of metal Ni particles thereby ensures their dispersion; increases the specific surface area as a result of the metal Ni phase creation enhancing the number of active sites, which is a precondition for improved electrochemical performance of the anode cermet.

The wet-chemical reduction mode using hydrazine is a cost-effective and energy-efficient

promising route for metal Ni incorporation in the BCY15 anode ceramic matrix providing homogeneity and uniform distribution of the nano-scaled metal Ni particles.

It may be concluded from this study that the cermet elaborated by ethylene glycol assisted approach possesses a capacity suitable to be used as anode in BCY-based pSOFC devices because of the anode ceramic matrix structure preservation and improved electrochemical performance in comparison with Ni-cermet prepared in water medium.

Acknowledgment: The research leading to these results has received funding from Bulgarian NSF under grant No E02/3/2014.

REFERENCES

1. N. Mahato, A. Banerjee, A. Gupta, S. Omar, K. Balani, *Prog. Mater. Sci.*, **72**, 141 (2015).
2. P. Frontera, V. Modafferi, F. Frusteri, G. Bonura, M. Bottari, S. Siracusano, P. Antonucci, *Int. J. Hydrogen Energy*, **35**, 11661 (2010).
3. H. Iwahara, T. Esaka, H. Uchida, N. Maeda, *Solid State Ionics*, **34**, 359 (1981).
4. H. Iwahara, H. Uchida, K. Ono, K. Ogaki, *J. Electrochem. Soc.*, **135**, 529 (1988).
5. H. Iwahara, *Solid State Ionics*, **52**, 99 (1992).
6. R. Bell, G. Millar, J. Drennan, *Solid State Ionics*, **131**, 211 (2000).
7. E. Fabbri, D. Pergolesi, E. Traversa, *Sci. Technol. Adv. Mater.*, **11** (2010) article 044301.
8. Z.-C. Chen, Y. Sakane, T. Tsurumaki, Y. Ayame, F. Fujita, Proceedings of 16th International Conference on Composite Materials, Kyoto, Japan, 2007, WeKM1-08_chenzc229918p.pdf.
9. B. Zhu, R. Raza, G. Abbas, M. Singh, *Adv. Funct. Mater.*, **21**, 2465 (2011).
10. Y. Li, C. Li, H. Wang, L. Li, Y. Qian, *Mater. Chem. Phys.*, **59**, 88 (1999).
11. Y. Moon, H. Park, D. Kim, C. Kim, *J. Am. Ceram. Soc.*, **78**, 2690 (1995).
12. H. Park, Y. Moon, D. Kim, C. Kim, *J. Am. Ceram. Soc.*, **79**, 2727 (1996).
13. J. Zhang, S. Yang, Q. Xue, *J. Mater. Res.*, **15**, 541 (2000).
14. D. P. Wang, D.-B. Sun, H.-Y. Yu, and H.-M. Meng, *J. Cryst. Growth*, **310**, 1195 (2008).
15. J. Park, E. Chae, S. Kim, J. Lee, J. Kim, S. Yoon, J.-Y. Choi, *Mater. Chem. Phys.*, **97**, 371 (2006).
16. G.-Y. Huang, S.-M. Xu, G. Xu, L.-Y. Li, L.-F. Zhang, *Trans. Nonferrous Met. Soc. China*, **19**, 389 (2009).
17. D. V. Goia, *J. Mater. Chem.*, **14**, 451 (2004).
18. M. Gabrovska, D. Nikolova, E. Mladenova, D. Vladikova, S. Rakovsky, Z. Stoyanov, *Bulg. Chem. Commun.*, **49**, Special Issue C, 171 (2017).
19. S.-H. Wu and D.-H. Chen, *J. Colloid Interface Sci.*, **259**, 282 (2003).
20. L. Kurihara, G. Chow, P. Schoen, *Nanostruct. Mater.*, **5**, 607 (2008).
21. H. Hu, M. Mo, B. Yang, X. Zhang, Q. Li, W. Yu, Y. Qian, *J. Cryst. Growth*, **258**, 106 (2003).
22. D. E. Vladikova, Z. B. Stoyanov, Z. Wuillemin, D. Montinaro, P. Piccardo, I. Genov, M. Rolland, *ECS Transactions*, **68**, 1161 (2015).
23. F. Rouquerol, J. Rouquerol, K. Sing, In Adsorption by Powders and Porous Solids, Principle, *Methodology and Applications*, Academic Press, New York, 1999.
24. M. Mogensen and S. Skaarup, *Solid State Ionic*, **86-88**, 1151 (1996).
25. J. Tong, D. Clark, L. Bernau, M. Sanders, R. O'Hayre, *J. Mater. Chem.*, **20**, 6333 (2010).

ВЪВЕЖДАНЕ НА Ni В АНОДНАТА КЕРАМИЧНА МАТРИЦА НА ПРОТОН ПРОВОДЯЩИ ТВЪРДООКСИДНИ ГОРИВНИ КЛЕТКИ: ЧАСТ II. МОКРА ХИМИЧНА РЕДУКЦИЯ В БЕЗВОДНА СРЕДА

М. В. Габровска^{1*}, Д. А. Николова¹, Е. А. Младенова², Д. Е. Владикова²,
С. К. Раковски¹, З. Б. Стойнов²

¹Институт по катализ, Българска академия на науките, ул. Акад. Г. Бончев, бл. 11, 1113 София, България
²Акад. Евгени Будевски Институт по електрохимия и енергийни системи, Българска академия на науките, ул. Акад. Г. Бончев, бл. 10, 1113 София, България

Постъпила на 26 май, 2017 г.; приета на 25 септември, 2017 г.

(Резюме)

Добре известният протон проводящ електролит итрий-дотиран бариев церат, $\text{BaCe}_{0.85}\text{Y}_{0.15}\text{O}_{2.925}$ (BCY15) е използван като анодна керамична матрица за синтез на Ni керамичен анод с приложение в протон проводящи твърдооксидни горивни клетки. Представен е рентабилен и енергийно-ефективен метод на мокра химична редукция при използване на никелов хлорид хексахидрат като прекурсор, етилен гликол като безводна среда, хидразин хидрат като редуциращ агент и алкален разтвор като регулатор на рН. Охарактеризирането на Ni кермет е извършено чрез прахова дифракция на рентгенови лъчи, нискотемпературна сорбция на азот и сканираща електронна микроскопия. Електрохимичните свойства са изследвани чрез импедансна спектроскопия след високотемпературно синтероване и редукция с водород. Установено е, че получаването на BCY15/Ni кермет в присъствие на етилен гликол води до (i) Запазване структурата на протон проводящата керамичната матрица от анодната композиция; (ii) Увеличаване на специфичната повърхност в резултат от образуване на металната никелова фаза, което е предпоставка за наличие на голям брой активни центрове за електрохимичното окисление на горивото; (iii) Получаване на хомогенни, нано-размерни, равномерно разпределени и не агломерирани метални никелови частици. Керметът, получен в среда на етилен гликол притежава качества, които го правят подходящ като анод в BCY15 протон проводящи твърдооксидни горивни клетки поради съхраняване структурата на анодната керамична матрица и неговото електрохимично поведение.

Ключови думи: BCY15/Ni аноден кермет, етилен гликол, хидразин, PXRD, SEM, Електрохимична импедансна спектроскопия